ELSEVIER Microelectronic Engineering 33 (1997) 241–248

MICROELECTRONIC ENGINEERING

W–CMP for sub-micron inverse metallisation

Herma van Kranenburg*, Herman D. van Corbach, Pierre H. Woerlee, Martin Lohmeier[1]

MESA Research Institute, University of Twente, P.O. Box 217, 7500 AE Enschede, Netherlands

---

Abstract

Chemical Mechanical Polishing (CMP) of tungsten for an inverse metallisation scheme is investigated. The influence of CMP parameters on removal rate and uniformity is studied. The main effects on the removal rate are the applied pressure and the rotation rate of the polishing pad. To the first order Preston's equation is obeyed. The uniformity is best with equal rpm of pad and wafer and with perforated pads. Also, pattern density effects of CMP of W/PETEOS are investigated. Dishing increased at larger W-linewidth. Oxide erosion increased at larger pattern density and smaller W-linewidth. Electrical measurements on submicron (0.4 and 0.5 μm) test structures yielded good CMP results.

---

1. Introduction

With decreasing dimensions of integrated circuits, the need for global planarisation increases. This is especially true in the back-end of the process where multiple layers of metal rapidly increase the topography. Interest in metal CMP in the inverse-metallisation process, where grooves are filled with metal and the metal outside the grooves is removed by CMP, is growing.

On an IC various dimensions of features occur (small contact plugs, variable groove width and space). This complicates a proper global planarisation and is the stimulus for the present systematical investigation of pattern density (PD) dependence.

In the present paper we will present characteristics of W-CMP. Removal rates and distribution across the wafers will be shown. Furthermore, the topography of structured W/PETEOS is studied after CMP. Finally, electrical results on polished half-micron structures are presented.

2. Experimental

All CMP experiments presented here were performed with an Al_2O_3-based slurry (commercially available) which is diluted with H_2O_2. After dilution the pH was measured to be 4.0. As polishing pads, we mainly used double-layers of a hard and soft pad, both non-perforated and perforated

---

*Corresponding author.

[1] Philips Research, Prof. Holstlaan 4, 5656 AA Eindhoven, the Netherlands

PII S0167-9317(96)00050-0

through the upper hard pad. Experiments were also done with a grooved hard pad on a soft foam layer. Pad-preconditioning was done prior to all CMP runs with a diamond tool. Cleaning of the wafers after CMP was done by a combination of DI water rinse, scrubbing using brushes and marangoni drying. The supply speed of the slurry was 125 ml/min. The rotation speed of the platen/pad and that of the wafer holder (hereafter referred to as head) were both varied between 25–75 rpm. The applied pressure was 300–700 g/cm^2, and at the back of the wafer a pressure (hereafter referred to as back pressure) of 0.1–0.3 bar was applied.

Tungsten was deposited by CVD on 150 mm Si wafers. The blanket W with a thickness of 800 nm was deposited with a $\sigma_1 < 3\%$.

Special CMP test structures were developed to investigate the CMP performance as a function of feature size and pattern density. The pattern density (PD) is defined as $L/(L+S)$, where L is the W-linewidth and S is the width of the oxide between two W-lines. For the structures the inverse metallisation process was used, in which first grooves were etched in plasma TEOS (PECVD), after which 20 nm Ti (PVD), 80 nm TiN (PVD) and a 900 nm thick CVD-W layer were deposited. The investigated structures include single lines, large areas (up to 500 μm square of W), plugs, systematically varied line/space patterns of several dimensions ($\mathrm{PD} = 0.2$–0.83, $L = 0.4$–100 μm) and (tapped) meander-comb structures of submicron width and several metres length ($L = 0.4$–0.5 μm, $S = 0.4$–0.6 μm, length ≤ 3.15 m).

The characterisation methods used are sheet resistance mapping (prometrix), profilometer (DEKTAK), optical microscopy, SEM, AFM, HP4145/HP4156. The removal rate is averaged over 49 points across each wafer. The uniformity, defined as

$$\frac{\text{maximum removed thickness} - \text{minimum removed thickness}}{2 \times \text{average removed thickness}}$$

is determined from a 49-points measurement on a diameter of 135 mm; the edge exclusion was 10%.

The W is removed by a combination of chemical and mechanical abrasion. The chemicals in the slurry react with W and form soluble WO_3 [1,2]. The contact of the W-surface with the pad and the Al_2O_3 particles in the slurry takes care of mechanical abrasion. Thus the combination of chemical and mechanical reaction yields a constant removal of the surface layer of the W. The oxide is not supposed to react with the used chemicals (selectivity) and is therefore mainly removed by mechanical abrasion. The degree to which the oxide is removed is measured by a parameter called erosion. Erosion is simply defined as the removed thickness of the (in this case) PETEOS in patterned areas. Since the W polishes faster than the TEOS, the TEOS supports nearby W-features and serves as a stopping layer for the CMP. This means that once the surface is nearly flat, the W close to the TEOS experiences less mechanical pressure than the W that is far from the TEOS. This gives rise to dishing: a different removed W-thickness adjacent to and far from the TEOS. The dishing increases with wider W-features, since this makes it easier for the pad to contact the W-surface [3]. We measured the dishing in the centre of the W-lines or W-areas, with the TEOS surface as the reference level.

3. Results and discussion

A DOE (design of experiments) technique was used to optimise the CMP process. The following CMP parameters were varied: applied pad temperature (288–313 K), applied pressure, back pressure and rotational speed of pad and head. It was found that the main effects on the removal rate are the applied pressure and the rotational speed of the polishing pad, while the other parameters only have a minor influence. In the first order Preston's equation (e.g. [4]) is obeyed, i.e. removal rate is proportional to the product of applied pressure and relative velocity between wafer and pad. The uniformity is lowest with equal rpm of pad and head. Furthermore, in order to attain good uniformities it was necessary to apply a pressure at the back of the wafer during CMP (0.2 bar was found to be an optimum). For realistic process conditions, typical removal rates are 150–250 nm/min and uniformities of 6–8% ($\equiv 1\ \sigma = 2$–5%) are reached, see Fig. 1. With the grooved pad higher removal rates were attained than with the perforated pad (similar to oxide-CMP [5]), however the uniformities were not as good. The non-perforated pad yielded the worst uniformity, which is probably caused by a bad slurry transport during CMP. The perforations and grooves in the other pads enable a better slurry transport, which especially improves the slurry amounts and refreshments between pad and wafer. CMP with the perforated pad yielded the most homogeneous polishing on the wafers, and therefore this pad was used for the experiments with the structured wafers. In Fig. 2 the distribution of the removal rate across the wafer is compared for the three investigated pads and these figures confirm the data on the uniformities.

The PD density effects of the wider features ($L = 5$–500 μm) were investigated by means of a profilometer. It was found that dishing increased at larger L and smaller PD, while oxide erosion increased at larger PD and smaller L, see Figs. 3–5. This can be understood as follows (e.g. [4,6,7]): 1) With increasing W-linewidth the distance from the centre of the W-features to the supporting TEOS increases, which enables a better contact between the pad and the W-surface. Thus the pad can exert higher pressure at the W-surface and material removal proceeds leading to an increase of dishing. 2) With increasing pattern density (PD) and equal W-linewidth (L), the width of the TEOS regions (S) decreases. Therefore the contact area of the pad and the TEOS parts decreases and thus the exerted pressure on the TEOS parts increases, which leads to a larger oxide erosion. 3) With increasing L and with equal PD, the width of the supporting TEOS regions increases and thus the erosion decreases. 4)

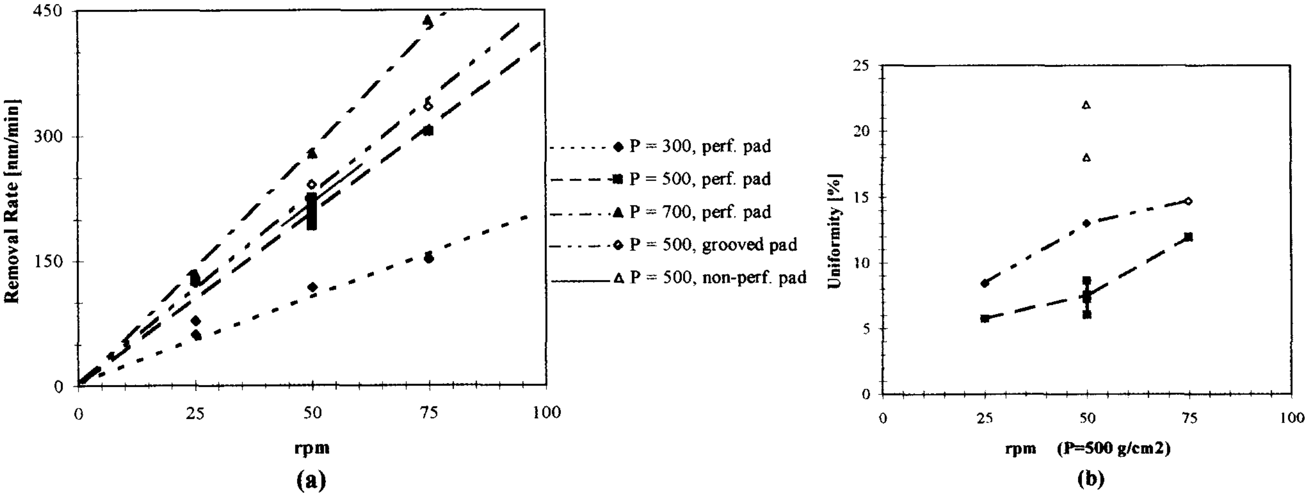

Fig. 1. Removal rate (a) and uniformity (b) as a function of CMP parameters (rpm pad = rpm head, applied pressure and pad type) determined from CMP on blanket W films.

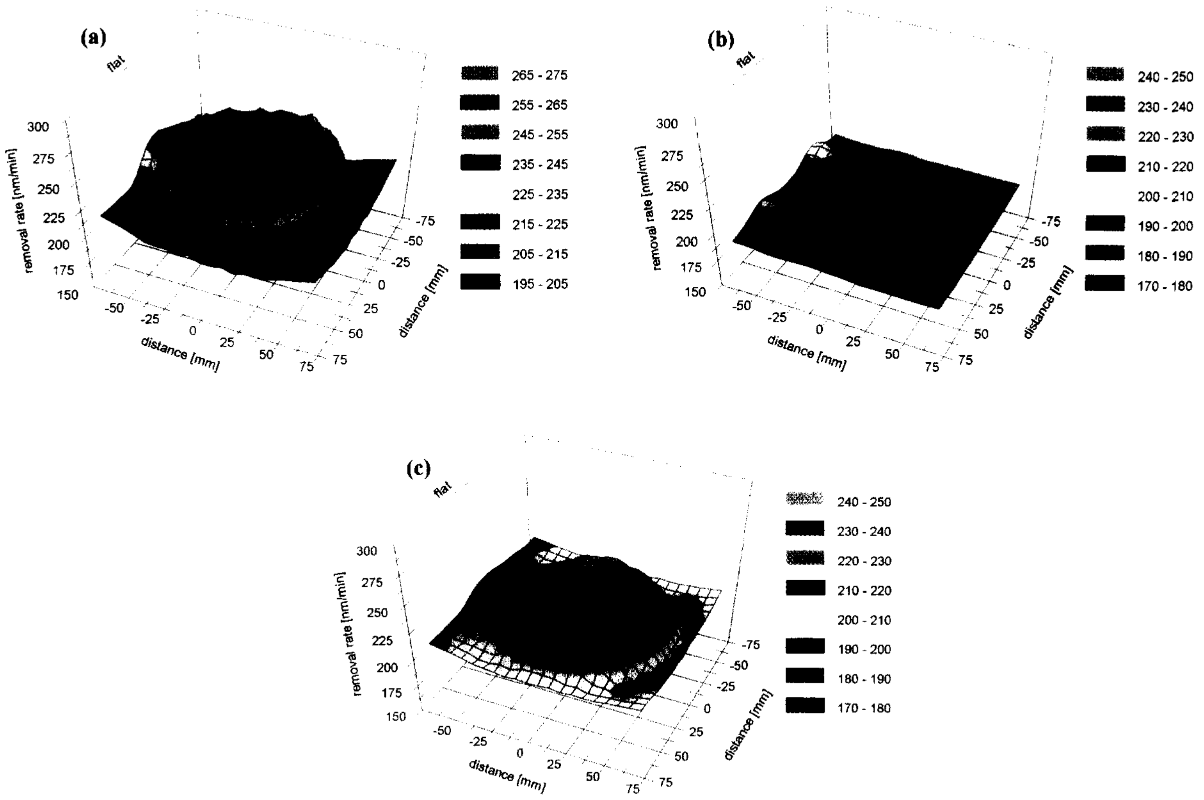

Fig. 2. Distribution of W-CMP removal rate on 150 mm wafers (note the extrapolation into a 150×150 mm^2 square) with rpm head = rpm pad = 50 and $P = 500$ g/cm^2. The performance of 3 pads is compared: (a) non-perforated, (b) perforated and (c) grooved.

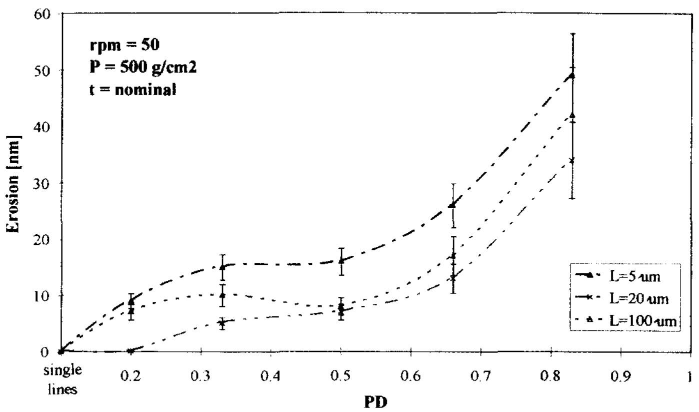

Fig. 3. Erosion as a function of pattern density. CMP was done at rpm head = rpm pad = 50 and $P = 500$ g/cm^2 and a nominal time.

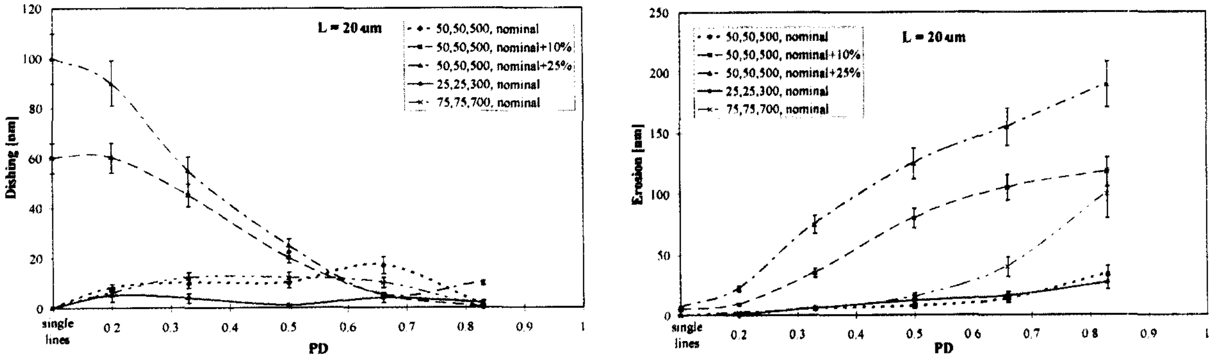

(a) (b)

Fig. 4. (a) Dishing and (b) erosion as a function of pattern density for a tungsten linewidth of 20 μm. Different CMP settings are compared: 50, 50, 500≡rpm = 50 and $P = 500$ g/cm^2 (nominal and overpolished); 25, 25, 300≡rpm = 25 and $P = 300$ g/cm^2; 75, 75, 700≡rpm = 75 and $P = 700$ g/cm^2. An estimation of errors is given in the error bars.

With increasing PD and equal L, the width of the TEOS regions decreases and this leads to a larger erosion. This larger erosion means that the reference level for determining the dishing gets lower, and thus a smaller dishing is found at higher PD. However, at large L and small PD, the remaining W-line thickness at the centre of the measured feature also decreases. In this case the two effects cancel each other, and a relative constant dishing as function of PD is found.

With nominal polishing time, the dishing and erosion is sufficiently small for the CMP settings rpm = 25 and $P = 300$ g/cm^2, and rpm = 50 and $P = 500$ g/cm^2, see Fig. 4. For the CMP setting rpm = 75 and $P = 700$ g/cm^2 the erosion increased significantly at large PD (at PD = 0.83 with nominal polishing, the erosion is 100–160 nm depending on the linewidth). Fig. 3 shows the erosion as a function of PD for several investigated linewidths for the CMP setting of rpm = 50 and $P = 500$ g/cm^2. At this setting the dishing was very low (less than 25 nm for all PD and L). Fig. 5 shows the dishing and erosion at the same CMP settings, but with 10% overpolishing time. It is obvious that both dishing and erosion increase rapidly with overpolishing time; dishing especially at large feature size (large L), and erosion especially at large PD (small S). The increase of dishing with overpolishing time, especially for large features is also found to occur at the large W areas (size up to 500 μm). The erosion of the adjacent large TEOS regions only slightly increases.

Dishing and erosion show interaction: when dishing is considerable the corners/edges of the TEOS (adjacent to the W) experience additional lateral polishing. (Similar to the lateral polishing components at the discontinuities in the Ti/TiN adhesion layer wherever there is a W structure [7].) Whereas with small dishing, and in the case of large areas and blanket films, polishing mainly proceeds through vertical polishing forces. Erosion can be further decreased by increasing the selectivity of the slurry. The selectivity of the slurry of W:PETEOS was measured (on blanket wafers at rpm = 50 and $P = 500$ g/cm^2) to be only 1:10.

With SEM, observation of the surface and cross-sections of the wafers are made. From SEM observations the surface appears to be very flat, see Fig. 6. With AFM measurements more details could be measured [8]. For submicron linewidths typical height differences between the W and TEOS

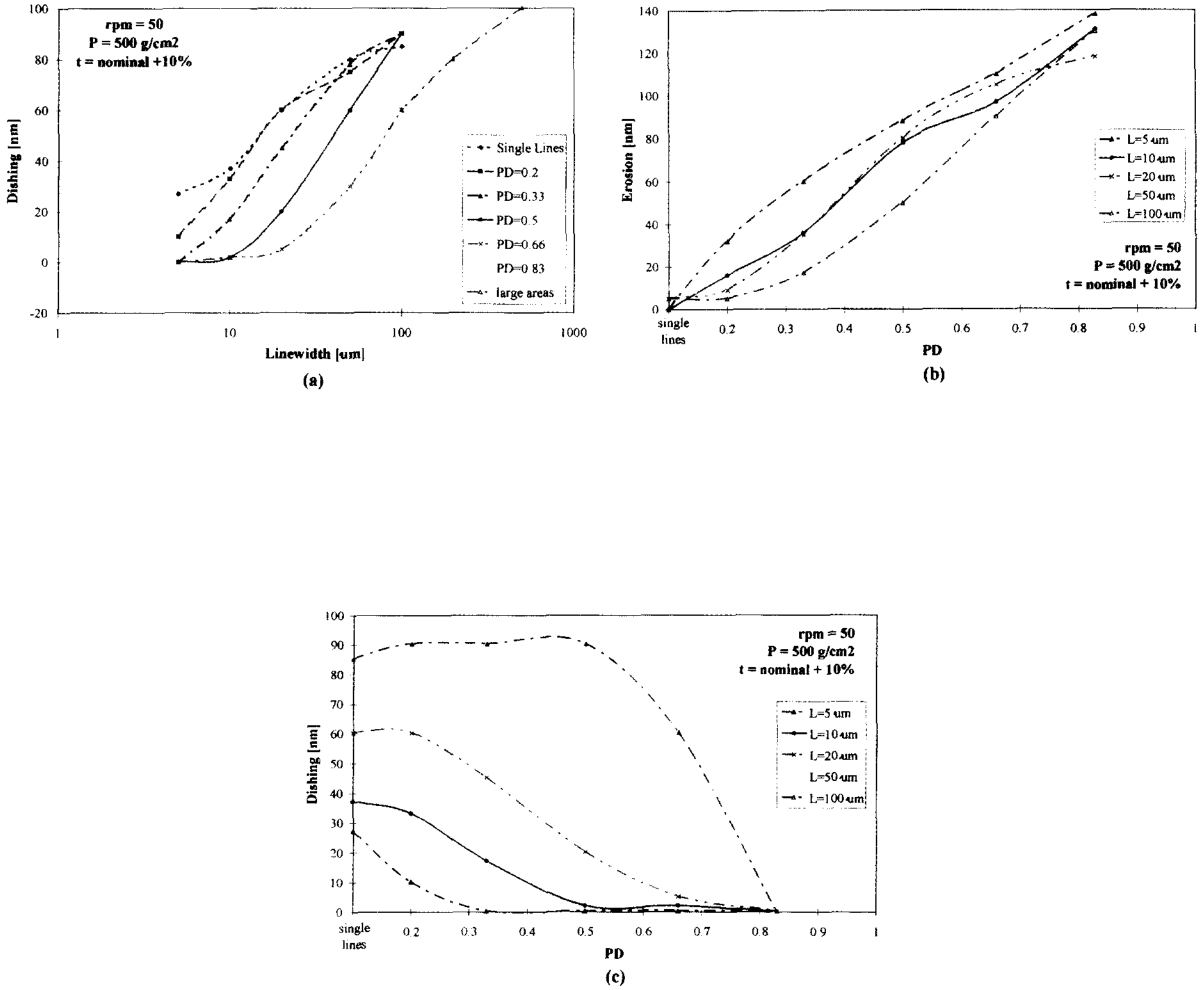

Fig. 5. (a) Dishing as a function of W-linewidth and (b) erosion and (c) dishing as a function of pattern density. CMP was done at rpm head = rpm pad = 50 and $P = 500$ g/cm^2 and with an overpolishing time of 10%.

were less than 5 nm. The surface roughness of W areas was larger than that of the TEOS areas. For W submicron linewidths the rms = 2.2 nm and better, for W features of 5 μm the rms roughness increased to 5.9 nm. On the TEOS very shallow scratches were present, in all directions and for all feature widths. These scratches are believed to be introduced by the CMP and can be removed by an oxide-buffing-step. On the TEOS typically rms = 0.2 nm was measured.

Electrical measurements were done on three different meander-comb structures, namely $L/S = 0.5/0.6$ μm, 0.4/0.5 μm and 0.4/0.4 μm. The total length of the meanders varied between 2.07 and 3.15 m. Both the continuity of the meander as a good isolation between meander and combs was established. For the rpm pad = rpm head = 50 and $P = 500$ g/cm^2 setting and the perforated pad this

Fig. 6. SEM cross-section of a 0.4 μm wide W-line with oxide width $S = 0.4$ μm.

was measured across the entire wafer, reflecting the good homogeneous distribution of the removal rate across the wafer. For example, for the rpm pad = rpm head = 75 and $P = 700$ g/cm^2 setting, the above mentioned electrical results were only obtained around the centre of the wafer. Nearer the edge of the wafer, due to the lower removal rate a lot of shorts were still present because not all W was removed. Fig. 7 shows the I–V curves for one meander-comb structure. The upper five curves are of

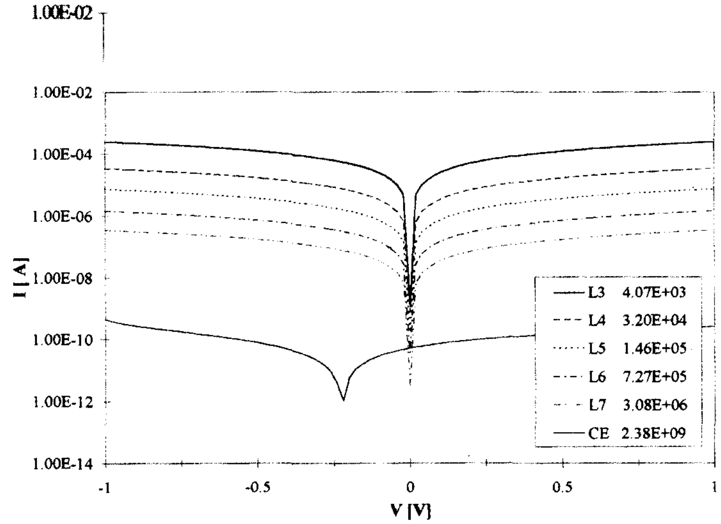

Fig. 7. I–V characteristics of a tapped meander with a total length of 3.15 m. $L/S = 0.4/0.5$ μm. In the legend the measured resistance is given in ohms. CMP was done at rpm head = rpm pad = 50 and $P = 500$ g/cm^2. L3 = 4.39 mm, L4 = 3.51 cm, L5 = 15.4 cm, L6 = 65.0 cm, L7 = 2.70 m and CE = 3.54 m comb–2.70 m meander.

various lengths, the lower one is measured between meander and comb. The latter one yielded a surface current due to poor surface passivation ($I < 1$ nA). The measured resistance quotients compare well to the length quotients of the meander, e.g. in Fig. 7: 7.9 (8), 35.9 (35), 179 (148) and 757 (615).

4. Conclusions

Good results on W-CMP have been shown, both with respect to removal rates and to uniformities. The PD effects were as follows: Dishing increased at larger W-linewidth and smaller pattern density. Oxide erosion increased at larger pattern density and smaller W-linewidth. However, the effects are sufficiently small for application in IC processing. Electrical characterisation using large meander comb structures shows high yield.

References

[1] F.B. Kaufman et al., *J. Electrochem. Soc.* **138** (1991) 3460.
[2] Chin-Wen Liu et al., *Proc. 1996 CMP-MIC Conference (1996)* 138.
[3] P. Burke, *Proc. VLSI Multilevel Interconnect Conference* (1991) 379.
[4] S. Sivaram et al., *Mat. Res. Soc. Symp.* **260** (1992) 511.
[5] M. Weling et al., *Proc. 1996 CMP-MIC Conference* (1996) 40.
[6] H. Landis et al., *Thin Solid Films* **220** (1992) 1.
[7] M. Rutten et al., *Proc. VLSI Multilevel Interconnect Conference* (1995) 491.
[8] V. Blaschke et al., *Proc. 1996 CMP-MIC Conference* (1996) 124.